

Development of a Dual Layered Dielectric-Loaded Accelerating Structure^{*}

Chunguang Jing¹, Alexei Kanareykin¹, Sergey Kazakov², Wanming Liu³, Elizaveta Nenasheva⁴, Paul Schoessow¹, and Wei Gai³,

¹. Euclid Techlabs, LLC, 5900 Harper Rd., Solon, OH 44139, U.S.A.

². KEK, Tsukuba, Japan

³. Argonne National Laboratory, 9700 S. Cass Ave, Argonne, IL 60439, U.S.A.

⁴. Ceramics Ltd., St. Petersburg, Russia

Abstract: RF power attenuation is a critical problem in the development of dielectric loaded structures for particle acceleration. In a previous paper [1] we suggested the use of a Multilayer Dielectric Loaded Accelerating Structure (MDLA) as a possible approach for reducing the rf losses in a single layer device. The MDLA is based on the principle of Bragg reflection familiar from optics that is used to partially confine the fields inside the dielectric layers and reduce the wall current losses at the outer boundary. We report here on the design, construction and testing of a prototype X-band double layer structure (2DLA). The measurements show an rf power attenuation for the 2DLA more than ten times smaller than that of a comparable single layer structure, in good agreement with the analytic results. Testing and operation of MDLAs also requires efficient power coupling from test equipment or rf power systems to the device. We describe the design and construction of two novel structures: a TM₀₃ mode launcher for cold testing and a power coupler for planned high gradient experiments.

1. Introduction

Although initial studies of using a dielectric loaded waveguide as a particle accelerating structure can be traced back to the early 1950's [2], intensive theoretical and experimental investigations of Dielectric-Loaded Accelerating (DLA) structures have been revived only in the past two decades [3-9]. Along with the progress that has been made toward a practical high gradient dielectric based accelerator, a few concerns have also arisen after a series of experimental studies [10-12] that have needed to be addressed. The relatively high field attenuation per unit length is an important factor limiting the efficiency of the conventional (single dielectric layer) structure [12, 13]. In our previous work [1] we proposed a solution, a multilayered DLA structure (MDLA), that can significantly reduce the rf losses compared to a single layer DLA structure while maintaining a comparable shunt impedance.

The conventional single layer DLA structure can be considered simply as a section of dielectric-lined circular waveguide with a conducting outer boundary (for transverse mode damping by modifying the boundary see [14, 15]) and an axial beam

^{*} The submitted manuscript has been created by UChicago Argonne, LLC, Operator of Argonne National Laboratory ("Argonne"). Argonne, a U.S. Department of Energy Office of Science laboratory, is operated under Contract No. DE-AC02-06CH11357. The U.S. Government retains for itself, and others acting on its behalf, a paid-up nonexclusive, irrevocable worldwide license in said article to reproduce, prepare derivative works, distribute copies to the public, and perform publicly and display publicly, by or on behalf of the Government.

channel. The TM_{01} accelerating mode possesses a strong magnetic field at the metal wall which in turn gives rise to large surface currents and hence large power attenuation. In general, this conductor surface current induced loss is much larger than the dielectric loss (assuming the loss tangent of the dielectric material used in DLA structures is in the range of 10^{-4} , typical for high quality microwave ceramic and polycrystalline materials [1,10,12]). For example, an X-band DLA structure that uses a Mg-Ti oxide based dielectric tube with 6mm ID, 9.1mm OD, dielectric constant of 20, and loss tangent of 1×10^{-4} will exhibit rf losses of 8.4dB/m, of which 6.6dB/m results from losses in the copper wall [13]. Instead of a simple uniform dielectric tube, the multilayered DLA structure shown in Fig.1 uses a dielectric tube that has radially alternating regions of high and low permittivity enclosed in a metal jacket. The multiple reflections from each boundary between two neighboring layers (Bragg Reflection) allow better localization of the accelerating mode electromagnetic fields along the waveguide axis and consequently a reduction in the wall losses caused by the magnetic field at the metal surface.

The idea of using Bragg reflection to construct an accelerator (the Optical Bragg Accelerator) has been previously analyzed in [16, 17]. The motivation for this was to design an all-dielectric accelerator (i.e. one that uses no outer metal jacket) since dielectrics are known to sustain higher electric fields than metals in the optical regime. (The all-dielectric accelerator design was proposed for optical frequencies and cannot be implemented for a microwave structure.) In another study, a five zone rectangular DLA structure was proposed [18] that uses two vacuum layers to reduce wall losses.

In this article, we present an experimental continuation of our previous theoretical study of MDLA structures [1]. We have developed an X-band dual layered DLA structure (2DLA) and experimentally demonstrated the use of Bragg reflection-based technology to reduce rf losses in dielectric loaded accelerators. Detailed design parameters of the structure are described in Section 2. Manufacture of the dual layer ceramic tube is given in Section 3. Section 4 presents the cold test setup, the design of a unique TM_{03} mode launcher, and the measurement results. A design of a high power TE_{10} - TM_{03} mode converter is discussed in Section 5.

2. Design of an X-band Dual Layered DLA Structure

The analytic solution for the electromagnetic fields in a multilayer structure is given in Appendix I. A more detailed description can be found in ref. [1]. In order to demonstrate the concept of using MDLA structures to reduce rf power losses, we began with the development of a dual layered DLA structure (2DLA). Generally, for a given RF frequency, a number of parameters such as the radius of the beam channel b_0 and the dielectric constants of each layer ϵ_i can be varied to achieve better acceleration properties (see Fig. A1). The thickness of each dielectric layer ($b_{i+1} - b_i$) is determined by Eq. (A3) and (A4) in Appendix and the synchronous condition (phase velocity equal to particle velocity, typically close to the speed of light, c). In our design, we chose 11.424GHz as the operating frequency; there has been considerable interest in X-band linear accelerators for high energy physics [NLC, CLIC] and high power X-band rf sources are becoming increasingly available [NRL,

SLAC]. The beam channel diameter is 6mm. The dielectric material of the inner layer is barium tantalite which has a dielectric constant of 37 and loss tangent of 3×10^{-4} ; the outer layer is alumina which has a dielectric constant of 9.7 and loss tangent of 1×10^{-4} .

Before construction, we calculated the properties of four different DLA structure designs including 1) a single layer DLA structure operating on the TM_{01} mode; 2) single layer, TM_{03} mode; 3) double layer, TM_{02} mode; and 4) double layer, TM_{03} mode. Their geometrical and accelerating parameters are given in Table 1. Comparing structures 1 and 3 one can see the total rf power loss drops from 26.4dB/m to 6.7dB/m, almost two orders of improvement. However, structure 3 uses the TM_{02} mode as the accelerating mode. This requires a larger volume of bulk dielectric loading, which in turn helps reduce overall DLA structure losses. A better comparison is structure 2 and structure 4, both operating at the TM_{03} mode. Table 1 shows that the dual layered TM_{03} mode DLA structure has a 3.9dB/m rf power loss that is ~ 13 times smaller than the single layer TM_{03} structure. Meanwhile, the shunt impedance, a measure of the effectiveness of producing an axial accelerating field for a given power dissipation, is also improved by factor 2 for the TM_{03} structure.

The shunt impedances of the four designs presented in Table 1 are considerably smaller by comparison with all-metal structures in the same frequency range [19]; however, the object here is not to demonstrate the advantages of dielectric based structures over all-metal cavities. Rather, the parameters of these structures are chosen to experimentally demonstrate the improvement in the rf attenuation using a multilayered dielectric tube. In addition, in contrast to a single layer DLA structure, the dielectric loss becomes the major contribution of the total loss for the MDLA structure. Further reduction in losses requires the development of new materials with very low loss tangents, for example high purity alumina, or polycrystalline CVD diamond with loss tangents $< 10^{-4}$ at X-band and extremely high rf breakdown limits [20, 21]. If the loss tangents of both materials used in the structures of Table 1 could be reduced to 0.5×10^{-4} , the shunt impedance of the dual layered TM_{02} mode structure would be improved to $27 M\Omega/m$ but the shunt impedance of the single layer TM_{01} mode structure to only $12 M\Omega/m$. We finally selected structure 4 (shown in the last column of Table 1) to be fabricated as the prototype 2DLA structure for these experiments.

(Note that the numerical prediction [22] of 2.7dB/m rf power loss in this structure assumed 1×10^{-4} as the loss tangent of the inner layer material. We have re-measured the loss tangent of the barium tantalite used in the 2DLA prototype structure and obtained $\sim 3 \times 10^{-4}$ for the loss tangent at 9.4GHz.)

Figure 1 shows the electric and magnetic fields of the X-band 2DLA structure simulated with the Microwave Studio® 3-D EM simulation tool. It can be clearly seen that the electromagnetic energy is localized within the first, high dielectric constant ceramic layer, which dominates the accelerating parameters like group velocity and shunt impedance. The combination of high permittivity of the inner layer and relatively low dielectric constant of the outer provides an energy concentration along the ceramic waveguide axis. One can see that the magnetic field near the

outside boundary of the outer layer dielectric tube is extremely low in Fig. 1(b). In turn this significantly reduces the surface current and so the copper wall losses that are the main contribution to the overall rf attenuation in a single layer DLA structure. For the MDLA, the major rf attenuation factor will be the loss tangent of the ceramic materials of the inner and outer layers insofar as the magnetic field magnitude is rather low at the surface of the copper sleeve of the MDLA structure.

3. Development of the Dual Layered Dielectric Tube

One of the key issues for the development of the 2DLA structure is the fabrication of high quality dual layered dielectric tubes. Based on the current technology for high quality factor microwave ceramic fabrication, the dual layered dielectric tubes that we used are constructed by sliding two separately fabricated dielectric tubes together. Two strict requirements for the dielectric tubes are the tight tolerances of the mechanical dimensions and the elimination of small deviations in the electrical properties such as the permittivity and loss tangent. In order to meet these requirements, Euclid Techlabs LLC in collaboration with Ceramic Ltd. [20] has developed an innovative press-form for hydraulic pressing of ceramic tubes. This technique makes it possible to place tubes inside a horizontal form that provides a high degree of uniformity of compaction along the length of the preformed sample. Furthermore, the double-stage ceramic tube forming process (a combination of hydraulic and isostatic pressing to produce dielectric tubes from 0.3~1.0 μm grain powders) has been used in the fabrication to ensure the homogeneous compression of the material along the tube length resulting in the uniformity of the waveguide dielectric parameters along the waveguide length. This technique significantly reduces the probability of macro-defects forming inside the bulk of the ceramic waveguide after the sintering process. Our preliminary studies show that the tube parameters are also significantly influenced by the technology of the thermal treatment and the sintering that the ceramic undergoes. The materials used to fabricate the dual layered dielectric tubes are alumina (dielectric constant = 9.7) for the outer layer, and a barium tetra-titanate-based oxide ceramic (dielectric constant = 37) for the inner layer. The final heat treatment of both materials is done at a temperature $T=600^\circ\text{C}$, and the optimal sintering temperatures are $T=1540^\circ\text{C}$ and 1280°C for alumina and barium tetra-titanate respectively.

Figure 2(a) shows the finished BaTi_4O_9 -based inner dielectric layer ($\epsilon_r=37$) and the Al_2O_3 based outer layer ($\epsilon_r=9.7$). The assembled dual layered dielectric tube is shown in Fig. 2(b). The mechanical gap between the inner and outer layers is defined by the surface finish of the dielectric tubes. The inner surface of the outer alumina layer is polished to an accuracy of 3 μm . However, any small gap that leads to a local field enhancement may cause breakdown under high power rf conditions [10]. In a 2DLA structure, there are only three field components, E_z , E_r , and H_ϕ present in the TM_{03} accelerating mode. At the boundary between the air gap and each dielectric layer, E_z has to be continuous and thus no field enhancement in the Z direction will appear. From Eq. (A4) in Appendix we know that E_z reaches a maximum along the radial direction at the outer surface of the inner dielectric layer and correspondingly E_r will

be zero since the following relation holds:

$$E_r = \frac{-j\beta}{k^2} \frac{\partial E_z}{\partial r} \quad (1).$$

Therefore, there will not be any significant field enhancement in the radial direction either. Figure 3 plots the analytic solution of the E-field (normalized to the accelerating gradient, E_z on axis) of the TM_{03} mode in the X-band 2DLA structure. An exaggerated gap (50 μm) is considered in the analysis where one can see that the field enhancement is rather low for the accelerating mode because the gap position is located at a node of the transverse electric field E_r [23]. The electric field enhancement ratio may be larger for the parasitic hybrid modes, but they can be easily damped [14, 15].

While fabricating the dual layered dielectric tubes we also made a few sample disks using the same fabrication procedure for measurements of the dielectric constant and losses. The measurements use a circular waveguide resonator with the sample disk completely filling the central section. Two movable mode launchers at both ends are used to excite axis-symmetric TE_{0mn} modes in the frequency range of 9-11GHz. These modes are characterized by a zero normal component of the electric field at the waveguide/sample boundary, eliminating the need for sample metallization. The parameters of these modes (resonant frequency and Q -factor) were used for the calculation of the dielectric properties of the sample under test including the dielectric constant and loss tangent. The error of the measurements of the dielectric response data are determined in turn by sample dimensional tolerances, resonant frequency stability, and quality factor measurement accuracy. Our measurements showed that the loss factor for the Al_2O_3 composition was $\leq 1 \times 10^{-4}$ at 9.4 GHz and the loss factor of $BaTi_4O_9$ did not exceed 3×10^{-4} at ~ 10 GHz. Meanwhile, the measured values of the dielectric constants were as expected 9.7 and 37.0 for the alumina and barium tetra-titanate respectively.

We fabricated five 7cm-long double layer ceramic tubes; four of which were used to build the X-band 2DLA structure by simply sliding the tubes into a 28 cm long circular copper waveguide. Under high power rf conditions, the longitudinal gap between two neighboring dielectric tubes may lead a serious dielectric breakdown [10]. A new ceramic brazing technology under development is expected to solve this problem [24]. For our low power tests we use these ‘identical’ double layer ceramic tubes to calibrate the bench test system and then obtain the rf loss of the X-band 2DLA structure.

4. Bench Testing

4.1 X-band TM_{03} mode launcher

A pair of TM_{03} mode launchers was developed as part of the cold test fixturing for the prototype 2DLA. The TM_{03} launcher is a device that transforms the TEM mode from the coaxial feed waveguide into the TM_{03} mode of the 2DLA structure while suppressing the excitation of any other modes. The same launcher attached to the downstream end of the structure will by reciprocity transfer the TM_{03} mode without reflection to the TEM mode of the output coaxial line. The TM_{03} launcher allows the

use of a vector network analyzer supplied with coaxial inputs for the power attenuation measurements.

That the basic design of the mode launcher and the way it applies to the 2DLA structure is shown in Fig. 4. It consists of a center conductor, two copper rings, and two tapered dielectric rings for impedance matching that include the inner BaTi₄O₉ ring and outer alumina ring. There is an air gap between the outer and inner copper rings. The presence of the copper rings along with the central conductor can split the original TEM wave into three overlaid TEM waves localized between the conductors. At the same time, the phase velocities of the waves in the ceramic and air gap regions are different so that it produces a phase shift between each region. With properly adjusted geometric factors the device can provide the desired phase shift to match the electromagnetic field pattern of the TM₀₃ mode at the input of the 2DLA structure. Therefore, only the TM₀₃ mode will be excited and the undesirable TM₀₁ and TM₀₂ modes at the same frequency will be suppressed.

3-D simulation plots of the magnetic field at different cross-sections shown in Fig. 5 provide a clear visualization of the TEM to TM₀₃ mode transition from a standard coaxial rf feed cable into the 2DLA structure. Figure 5(a) shows the azimuthal magnetic field for the TEM mode of the coaxial waveguide. Figure 5(b) is the magnetic field in the mode launcher that matches the field pattern of the TM₀₃ mode in the double layer DLA structure, shown in Figure 5(c). The color maps indicating the field strengths are plotted logarithmically in Fig. 5(b) and Fig. 5(c) in order to display the extremely weak magnetic field in the outer dielectric layer.

The S-parameters of the TM₀₃ launcher have also been simulated (see Fig. 6). The simulation is configured as an input TM₀₃ mode launcher (TEM to TM₀₃), a 2DLA structure (7cm long), and a reverse positioned TM₀₃ mode launcher (TM₀₃ to TEM). The simulation results (neglecting dielectric and copper losses) show good impedance matching with S₁₁ = -20.7 dB and S₂₁ = -0.03 dB at 11.424GHz; and a bandwidth of 50 MHz for S₁₁ < -15dB centered at 11.424GHz. We also simulated the case with induced air gaps between the mode launcher and double layer DLA structure, which is the normal situation during bench testing. The rf response was not found to be significantly affected. Two sets of TM₀₃ mode launchers have been fabricated. A complete TM₀₃ mode launcher assembly is shown in Fig. 7. The large copper support before the mode launcher fixes the center conductor on axis.

4.2 Bench test of the X-band dual layered DLA structure

The bench test of the 2DLA structure was performed at Argonne National Laboratory, where we used a HP8510C Vector Network Analyzer and the TM₀₃ mode launchers to characterize its rf properties (basically rf transmission and reflection) within the operational frequency range. During the measurement, we first tested the structure with only one 7cm ceramic waveguide loaded. The results obtained have been used as our baseline for calibration of the TM₀₃ mode launcher. Then we loaded a second 7cm section of double layer ceramic tube, and measured both the transmission and reflection coefficients again. The subtracted value of the transmission was the calibrated rf loss factor value for the 7 cm dual layer DLA

structure. Very low rf reflections were observed in both cases.

Measurement results for a single section of double layer waveguide are presented in Fig. 8; simulation results are plotted for comparison. One can see that both simulation and experimental data are in a very good agreement except for a larger transmission value predicted by the simulation than we experimentally measured. This difference occurs because the rf losses of the copper section and dielectrics as well as slight mismatches between the mode launcher and 2DLA structure were not taken in to account in the simulation. For one section of ceramic tube, $S_{21} = -1.08\text{dB}$ at 11.424 GHz; for 2 pieces, $S_{21} = -1.35\text{dB}$. Both cases have very low S_{11} (less than -15dB). Therefore, the transmission loss of one 7 cm long section of dual layer ceramic waveguide is 0.27dB. Based on this result, the power attenuation is less than 4dB/m for the X-band double layer ceramic-based accelerator.

4.3 Discussion

The measured 4dB/m rf attenuation agrees very well with the theoretical estimation of 3.9 dB/m obtained previously, where we assumed the loss factor of barium tetra-titanate is 3×10^{-4} for the inner DLA layer. Ideally, the rf loss of our baseline measurement (S_{21} of a single section of double layer ceramic tube) should be 0.27dB as well. However, the matching between the TM_{03} mode launcher and 2DLA structure was not perfect, causing the reduction of S_{21} of a single segment of double layer ceramic tube by -1.08dB . However, possible mismatching between neighboring dual layer dielectric sections was found to be negligible as long as they were firmly pressed together to obtain good mechanical and electrical contact.

5 Design of the High Power TE_{10} - TM_{03} Mode Converter

To be able to accelerate particles using an externally powered MDLA structure, a high power rf coupler is needed to efficiently transform the TE_{10} mode of the rf source's rectangular output waveguide to the TM_{0n} mode of the cylindrical DLA structure. One possible solution is to break this mode conversion into two steps, a TE_{10} - TM_{01} converter and a TM_{01} - TM_{0n} mode converter. The TE_{10} - TM_{01} mode converter has been successfully tested [25, 26]; here, we use the X-band dual layered TM_{03} mode DLA structure as an example to briefly introduce the design of the TM_{01} - TM_{0n} mode converter. (We note that this is a different device from the mode launcher discussed in Sect. 4.1, which is used to convert a TEM mode from a coaxial cable to a TM_{03} .)

This converter is based on the dielectric loaded corrugated waveguide shown in Fig. 9, where a double layer dielectric tube is inserted in a corrugated waveguide for matching the impedance. The periodically varying radius of the corrugated waveguide provides the mode transformation from the TM_{01} to the TM_{03} cylindrical waveguide mode. In principle, any non-uniformity along the waveguide, such as a varying radius or axis bending in the circular waveguide will lead to energy exchange among the various guided wave modes resulting in mode transformation of the propagating rf wave. As long as the azimuth angle does not change and the radius varies along the axis of a circular waveguide, the transverse magnetic mode TM_{mn} can be converted

only into another transverse magnetic TM_{mn} mode. In addition, to build up a directional mode conversion between two specific modes and simultaneously suppress others, a periodic geometric perturbation along the waveguide must be established, and its period λ_w must satisfy the following equation:

$$\Delta\beta = \beta_1 - \beta_2 = l \frac{2\pi}{\lambda_w} \quad l = \pm 1, \pm 2, \dots \quad (2)$$

where β_i is the propagation constant of the i^{th} mode. For $l=1$, the period of the geometric perturbation is the beat wavelength of the two converted modes; under this condition the energy of the new mode increases as both modes propagate along the waveguide. The length of the mode converter is $L = N\lambda_w$, where $N=1, 2, \dots$ is determined by the required transfer efficiency, frequency bandwidth, and perturbation strength.

Figure 10 shows the simulation results for a TM_{01} - TM_{03} mode converter, which has $N=6$ and $\lambda_w=15.4$ mm. Instead of using a corrugated copper housing, we modeled a corrugated outer layer ceramic tube for the simulation, which has an equivalent effect. The predicted conversion efficiency has reached 95% within the pass band for TM_{01} - TM_{03} mode transformation, and the TM_{02} mode has been effectively suppressed.

6 Summary

The relatively large rf losses caused by surface currents at the conducting boundary of a dielectric accelerating structure can be reduced significantly through the use of multiple dielectric layers to form a Bragg structure. We have successfully designed, built and tested an X-band double layer structure that demonstrated a -22 dB/m reduction in rf attenuation compared to a single layer device. Mode conversion devices that are necessary for efficient coupling of rf from a rectangular waveguide into the dual layer structure were also demonstrated. The bench testing of the fabricated multilayer DLA structure has been carried out, and the experimental results are presented. Finally, feasibility of the Bragg reflection approach for the dielectric based accelerating structure development has been demonstrated.

Acknowledgement

This work is supported by US DOE SBIR Phase I funding under Contract No. DE-FG02-05ER84356.

Appendix I. Electromagnetic fields in a Multilayer Dielectric Structure

Consider the MDLA structure shown in Fig.A1. General solutions for the electric and magnetic fields for the i^{th} dielectric layer are

$$\begin{aligned}
E_{z_i}(z, r, \phi) &= [A_i J_m(k_i r) + B_i Y_m(k_i r)] e^{jm\phi} e^{j(\omega t - \beta z)} \\
E_{r_i}(z, r, \phi) &= \left[A_i \frac{-j\beta}{k_i} J'_m(k_i r) + B_i \frac{-j\beta}{k_i} Y'_m(k_i r) + C_i \frac{m\omega\mu_i}{k_i^2 r} J_m(k_i r) + D_i \frac{m\omega\mu_i}{k_i^2 r} Y_m(k_i r) \right] e^{jm\phi} e^{j(\omega t - \beta z)} \\
E_{\phi_i}(z, r, \phi) &= \left[A_i \frac{m\beta}{k_i^2 r} J_m(k_i r) + B_i \frac{m\beta}{k_i^2 r} Y_m(k_i r) + C_i \frac{j\omega\mu_i}{k_i} J'_m(k_i r) + D_i \frac{j\omega\mu_i}{k_i} Y'_m(k_i r) \right] e^{jm\phi} e^{j(\omega t - \beta z)} \\
H_{z_i}(z, r, \phi) &= [C_i J_m(k_i r) + D_i Y_m(k_i r)] e^{jm\phi} e^{j(\omega t - \beta z)} \\
H_{r_i}(z, r, \phi) &= \left[A_i \frac{-m\omega\varepsilon_i}{k_i^2 r} J_m(k_i r) + B_i \frac{-m\omega\varepsilon_i}{k_i^2 r} Y_m(k_i r) + C_i \frac{-j\beta}{k_i} J'_m(k_i r) + D_i \frac{-j\beta}{k_i} Y'_m(k_i r) \right] e^{jm\phi} e^{j(\omega t - \beta z)} \\
H_{\phi_i}(z, r, \phi) &= \left[A_i \frac{-j\omega\varepsilon_i}{k_i} J'_m(k_i r) + B_i \frac{-j\omega\varepsilon_i}{k_i} Y'_m(k_i r) + C_i \frac{m\beta}{k_i^2 r} J_m(k_i r) + D_i \frac{m\beta}{k_i^2 r} Y_m(k_i r) \right] e^{jm\phi} e^{j(\omega t - \beta z)}
\end{aligned} \tag{A1}$$

where

$$k_i = \omega \sqrt{\frac{\mu_{ri} \varepsilon_{ri}}{c^2} - \frac{1}{v_p^2}} \tag{A2}$$

$$\beta^2 = \omega^2 \mu_0 \varepsilon_0 \mu_{ri} \varepsilon_{ri} - k_i^2$$

v_p is the phase velocity of the wave, c is the speed of light in vacuum, k_i is the transverse wave number in the i^{th} layer, β is the propagation constant along the z axis, and μ_{ri} and ε_{ri} are respectively the relative permeability and permittivity for the i^{th} layer. A_i , B_i , C_i and D_i are four to-be-solved unknown coefficients for each layer in which B_0 and D_0 are zero to satisfy the boundary condition at $r=0$.

All the unknown coefficients are related through a recurrence relation from the i^{th} layer to the $(i+1)^{\text{th}}$ layer

$$\begin{pmatrix} A_{i+1} \\ B_{i+1} \\ C_{i+1} \\ D_{i+1} \end{pmatrix} = M_i \begin{pmatrix} A_i \\ B_i \\ C_i \\ D_i \end{pmatrix} \tag{A3}$$

where M_i , ($i=0, 1, \dots, N$) is a 4 by 4 transfer matrix for the i^{th} boundary [1, 27]. Since B_0 and D_0 are zero, we then have $(4 \times N) + 2$ unknowns for a N layer structure. Therefore, with two additional equations we can solve Eq. (A3). Two equations imposed at the boundary of each layer are

$$\begin{cases} H_\phi(r=b_i) = E_z'(r=b_i) = 0 & \text{if } k_{i+1} < k_i \\ H_\phi'(r=b_i) = E_z(r=b_i) = 0 & \text{if } k_{i+1} > k_i \end{cases} \tag{A4}$$

which can establish Bragg reflections among the dielectric layers and confine most of the EM energy in the vacuum channel ($r < r_0$). The outmost boundary conditions at inner surface of the metallic sleeve are $E_z(r=b_N) = H_r(r=b_N) = 0$ and ensure that the rf energy is confined to the interior of the DLA. The condition for a non-trivial solution to Eq. (A3) and (A4) will determine the dispersion relation of this MDLA

structure. By normalizing either the initial electric or magnetic field and combining with Eq. (A2) the ω - β relation for the different modes can be found. Modes supported by the MDLA structure are HEM_{mn} modes, TM_{0n} and TE_{0n} modes, where m refers to the order of the Bessel functions comprising the eigensolution and n is the different number of their roots. In general the TM_{0N} mode is chosen to be the accelerating mode in the N-layered DLA structure.

References

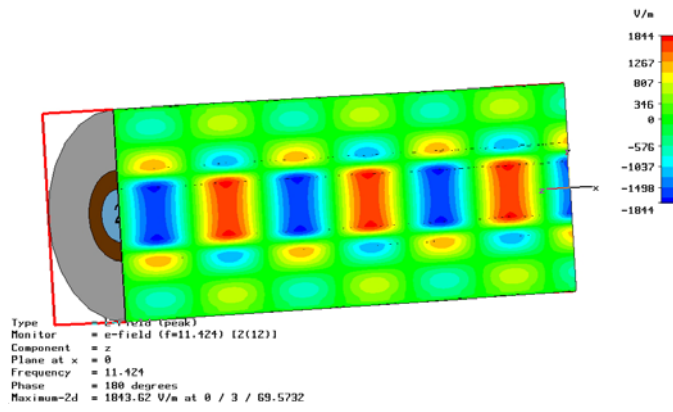
- [1] C. Jing, W. Liu, W. Gai, J. Power and T. Wong. Nucl. Instr. Meth. in Phys. Research. A, v. 539, (2005) 445-454.
- [2] G. Flesher and G. Cohn. AIEE Trans. 70 (1951) 887-893.
- [3] T. Zhang. Proc. 7th AAC Workshop, AIP Conf. Proc. 398 (1996)
- [4] W. Gai, P. Schoessow, B. Cole, R. Konecny, J. Norem, J. Rosenzweig, and J. Simpson. Phys. Rev. Lett. (1988) 2756-2759.
- [5] P. Schoessow, M. Conde, W. Gai, R. Konecny, J. Power, and J. Simpson. J. App. Phys. 84 (1998) 663
- [6] A. Tremaine, J. Rosenzweig, and P. Schoessow. Phys. Rev. E 56 (1997) 7204.
- [7] T. Zhang, J. Hirshfield, T. Marshall, and B. Hafizi. Phys. Rev. E 56 (1997) 4647-4655.
- [8] D. Yu, D. Newsham, and A. Smirnov. Proc. 10th AAC workshop, AIP Conf. Proc. 647 (2002) 484-505.
- [9] M. Hill, C. Adolphsen, W. Baumgartner, R. Callin, X. Lin, M. Seidel, T. Slaton, and D. Whittum. Phys. Rev. Lett. 87 (2001) 094801.
- [10] C. Jing, W. Gai, J. Power, R. Konecny, S. Gold, W. Liu and A. Kinkead *IEEE, Trans. PS*, vol.33 No.4, (2005)1155-1160.
- [11] J. Power, W. Gai, S. Gold, A. Kinkead, R. Konecny, C. Jing, W. Liu, and Z. Yusof. Phys. Rev. Lett. 92.16 (2004) 164801.
- [12] P. Zou, W. Gai, R. Konecny, X. Sun, T. Wong, and A. Kanareykin. Rev. Sci. Instr. 71, 6 (2000) 2301-2304.
- [13] P. Zou PhD Dissertation, Illinois Inst. Tech. 2001.
- [14] E. Chojnacki, W. Gai, C. Ho, R. Konecny, S. Mtingwa, J. Norem, M. Rosing, P. Schoessow, and J. Simpson, *J. Appl. Phys.*, **69**(9), 1991, pp.6257-6260.
- [15] W. Gai and C. Ho, *J. Appl. Phys.*, **70**(7), 1991, pp.3955-3957.
- [16] L. Schachter, R. L. Byer, and R. H. Siemann, Phys. Rev. E **68** 036502 (2003)
- [17] Mizrahi, L. Schachter, R. L. Byer, and R. H. Siemann, Proc. PAC03 (2003) 728-730.
- [18] C. Wang, V. Yakovlev, J. Hirshfield. Proc. PAC05 (2005) 1282-1284.
- [19] SLAC Report 474, 1996.
- [20] <http://www.euclidtechlabs.com>
- [21] A. Kanareykin, C.-J. Jing, P. Schoessow, M. E. Conde, W. Gai, R. Gat. Proceedings Particle Accelerator Conference PAC2007, Albuquerque, NM, pp. 3163-3165, 2007.
- [22] C. Jing, A. Kanareykin, and S. Kazakov. Proc. 2007 PAC, (2007) 3160-3162

- [23] A. Altmark, A. Kanareykin, *Technical Physics Letters*. v.34, # 2, pp.174-176, 2008.
- [24] R. W. Bruce, R. L. Bruce, A. W. Fliflet, M. Kahn, S. H. Gold, A. K. Kinhead, D. Lewis, III, and M. A. Imam *IEEE Tran. Plasma Sci.* 33, 2, (2005) 668-678.
- [25] W. Liu, C. Jing, W. Gai, R. Konecny and J. Power. *Proc. PAC03*, (2003) 1810-1812.
- [26] C. Jing, PhD Dissertation, Illinois Inst. Tech. 2005.
- [27] P. Yeh and A. Yariv. *J. Opt. Soc. Am.* 68 (1978) 1196.

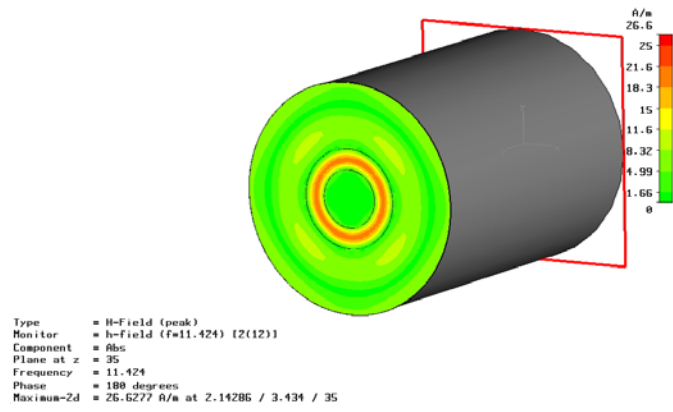
Table 1

Comparison of the geometrical and accelerating parameters for different 11.424GHz DLA structures and operating modes. The structure shown in the last column (bold) has been constructed; measurements of its electronic characteristics are reported here.

	Single layer TM ₀₁ mode	Single layer TM ₀₃ mode	Dual layer TM ₀₂ mode	Dual layer TM₀₃ mode
Group velocity	0.031c	0.028c	0.048c	0.064c
Shunt impedance (MΩ/m)	8.9	3.8	9.5	8.4
r/Q (Ω/m)	6987	1553	2916	2040
rf Power ATTN (dB/m)	26.4	15.2	6.7	3.9
ε ₁ (loss tangent)	37(3×10 ⁻⁴)	37(3×10 ⁻⁴)	37(3×10 ⁻⁴)	37(3×10⁻⁴)
ε ₂ (loss tangent)			9.7(1×10 ⁻⁴)	9.7(1×10⁻⁴)
b ₀ – b ₁ – b ₂ (mm)	3 – 4.13	3 – 8.49	3 – 5.17 – 7.57	3 – 5.17 – 12.02

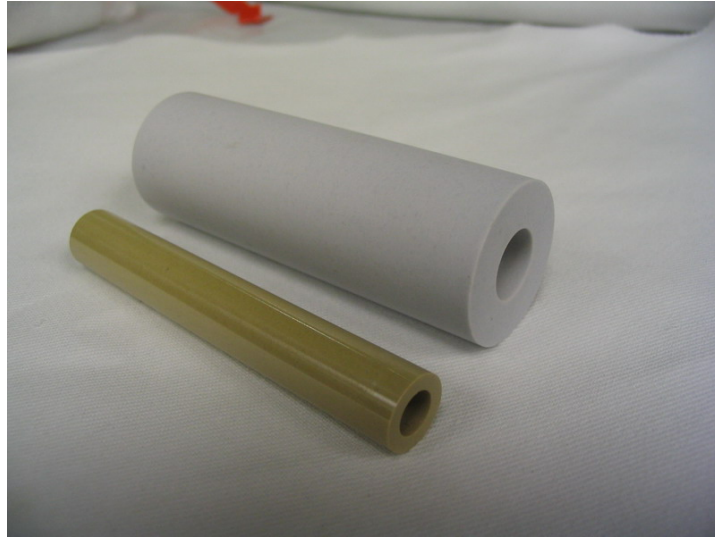


(a)

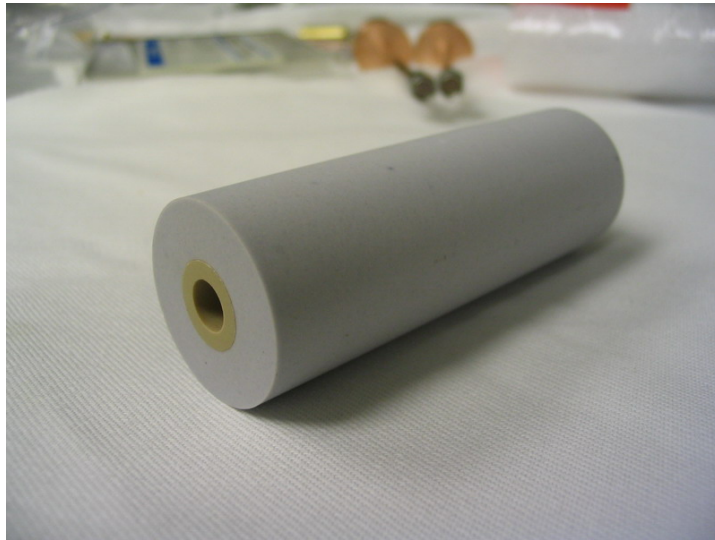


(b)

Figure 1. Electromagnetic field distribution in the X-band 2DLA structure simulated with Microwave Studio®: (a) E-field magnitude; (b) H-field magnitude.



(a)



(b)

Figure 2. (a) The BaTi_4O_9 -based inner dielectric layer ($\epsilon_r=37$) and the Al_2O_3 based outer layer ($\epsilon_r=9.7$) before assembling; (b) the assembled dual layer dielectric tube.

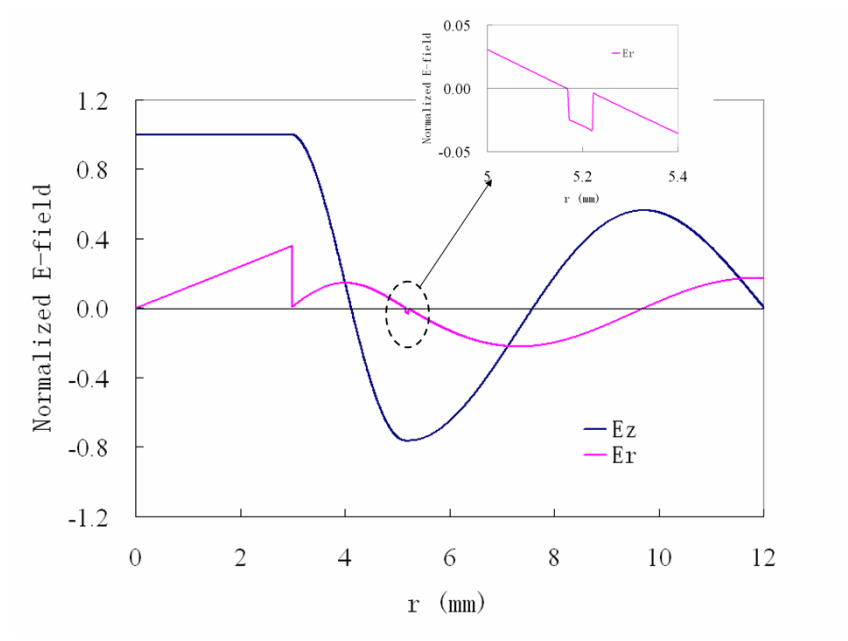


Figure 3. Longitudinal and transverse electric field profiles of the TM_{03} mode in the X-band 2DLA structure. The parameters of the structure are shown in the last column of Table 1.

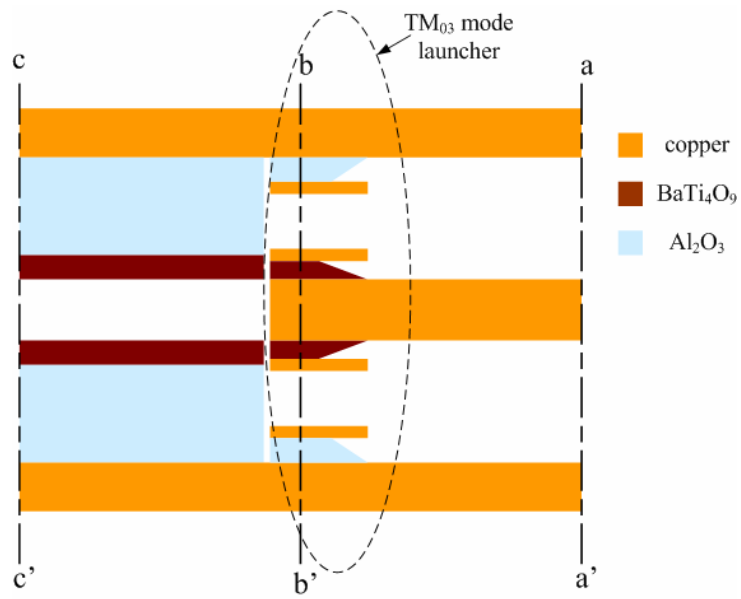


Figure 4. Schematic cross sectional drawing of the X-band TEM-TM₀₃ mode launcher for the 2DLA structure. Three cross sectional cut-planes, a-a', b-b', and c-c', are marked to show the magnetic field patterns at different locations in Fig. 5.

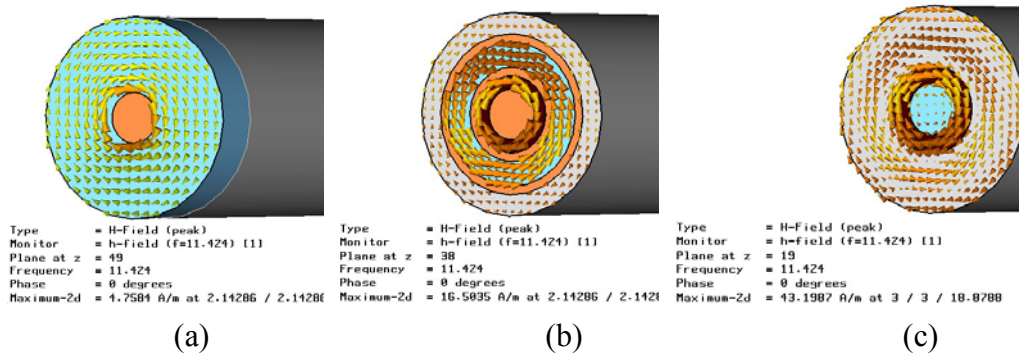


Figure 5. Magnetic field patterns of mode launcher and 2DLA structure along cross sections at different axial positions: (a) input of the mode launcher (see a-a' plane in Fig.4); (b) middle of the mode launcher (see b-b' plane in Fig.4); (c) middle of the 2DLA structure (see c-c' plane in Fig.4). Simulation is performed using CST Microwave Studio®. Color legend: Copper (orange), alumina (grey), barium tetra-titanate (dark brown), air (blue); background material is a perfect electrical conductor.

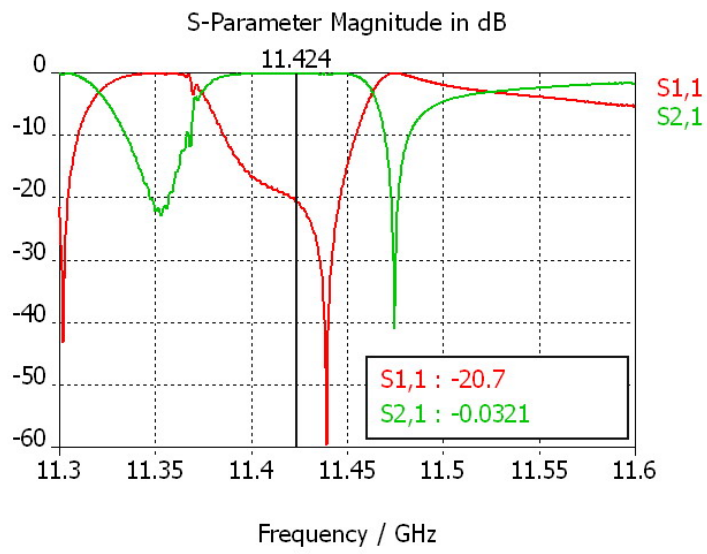


Figure 6. Simulated S-parameters of the 2DLA structure with TM_{03} mode launchers at both ends.



Figure 7. The assembled X-band TEM-TM₀₃ mode launcher.

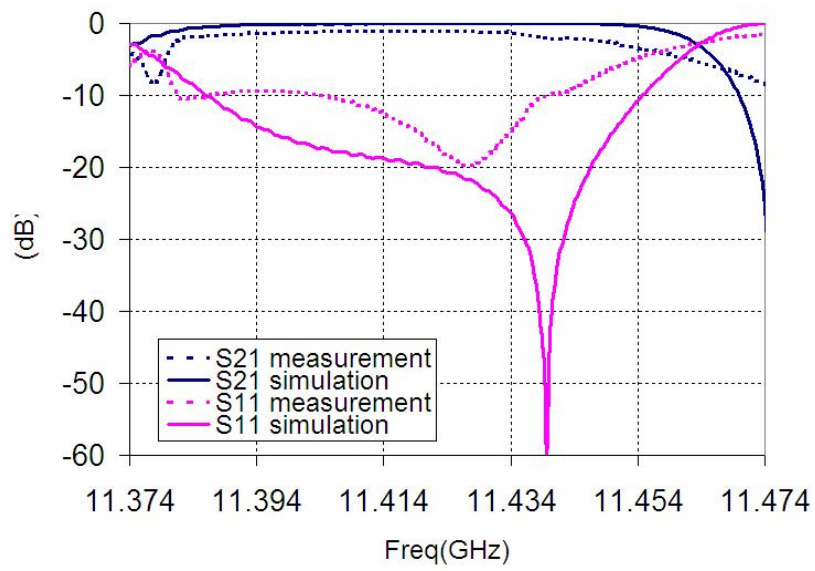


Figure 8. Comparison of the results of the bench testing and simulation of the structure with a single section of double layer ceramic tube.

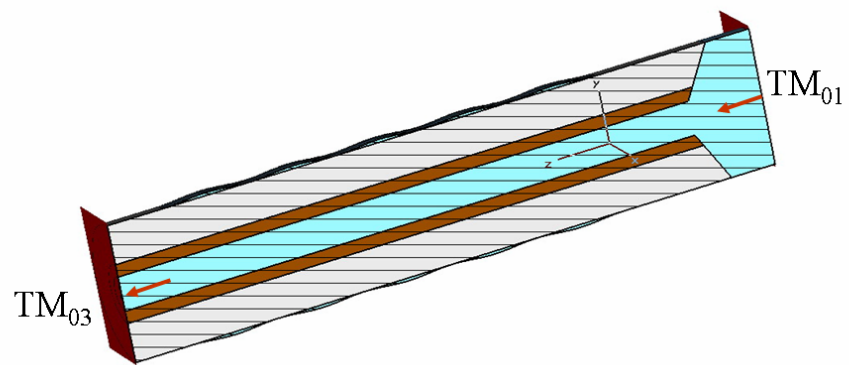


Figure 9. Cross section of dielectric loaded, corrugated waveguide based TM_{01} - TM_{03} mode converter.

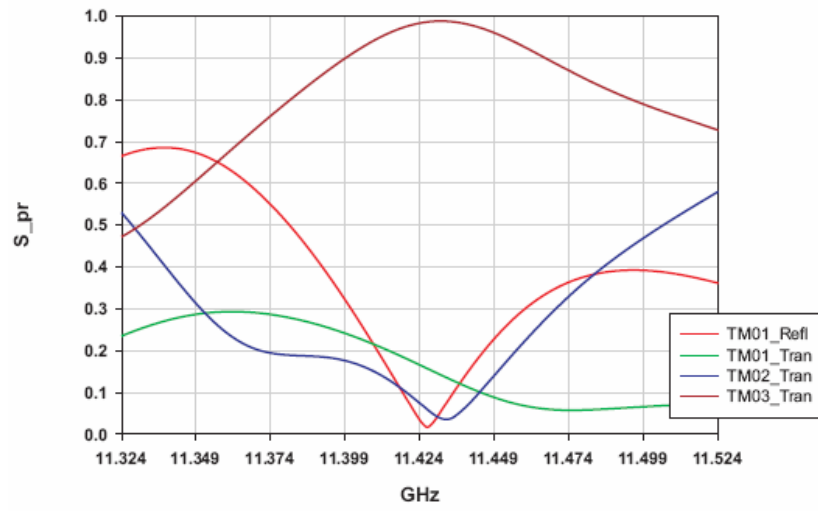


Figure 10. Simulation results for the TM₀₁-TM₀₃ mode converter (S-parameters are shown on a linear scale).

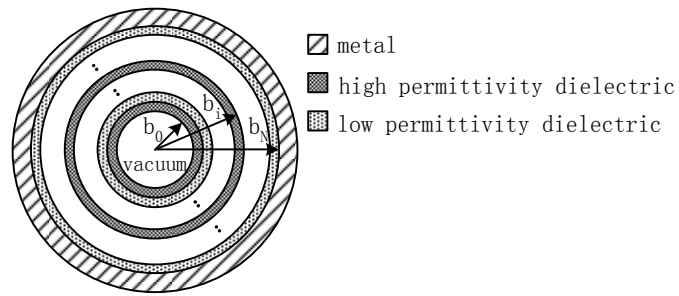


Figure A1. Cross-section of the multilayer dielectric-loaded accelerating (MDLA) structure. The structure is cylindrical waveguide which consists of a vacuum core with radius b_0 surrounded by alternating high and low permittivity dielectric tubes with outer radius b_i , enclosed in a conducting jacket.

